Research Article

EASL EUROPEAN ASSOCIATION FOR THE STUDY OF THE LIVER | JOURNAL OF HEPATOLOGY

OV6$^+$ tumor-initiating cells contribute to tumor progression and invasion in human hepatocellular carcinoma

Wen Yang[1,†], Chao Wang[1,†], Yan Lin[1,†], Qiong Liu[1,†], Le-xing Yu[1], Liang Tang[1], He-Xin Yan[1], Jing Fu[1], Yao Chen[1], Hui-Lu Zhang[1], Liang Tang[1], Long-Yi Zheng[1], Ya-Qin He[1], Yu-Qiong Li[1], Fu-Quan Wu[1], Shan-Shan Zou[1], Zhong Li[1], Meng-Chao Wu[1], Gen-Sheng Feng[1], Hong-Yang Wang[1,2,*]

[1]*International Cooperation Laboratory on Signal Transduction, Eastern Hepatobiliary Surgery Institute, Second Military Medical University, Shanghai 200438, PR China;* [2]*State Key Laboratory of Oncogenes and Related Genes, Shanghai Cancer Institute, Renji Hospital, Shanghai Jiaotong University School of Medicine, Shanghai 200032, China*

Background & Aims: Accumulating evidence suggests the involvement of tumor-initiating cells (T-ICs) in cancer genesis, but whether liver T-ICs contribute to HCC invasion and metastasis remains unclear.

Methods: OV6$^+$ T-ICs were isolated from SMMC7721 and HuH7 cell lines by magnetic sorting. Characteristics of T-ICs were assessed by *in vitro* and mouse xenograft assays. Expression of OV6 was determined by immunostaining in specimens from 218 HCC patients, and Kaplan–Meier survival analysis was used to determine the correlation of OV6 expression with prognosis.

Results: OV6$^+$ T-ICs isolated from HCC cell lines not only possess a higher capacity to form tumor spheroids *in vitro*, but also had a greater potential to form tumors when implanted in non-obese diabetic/severe combined immunodeficient mice, suggesting their elevated self-renewal capacity and tumorigenicity. Moreover, OV6$^+$ T-ICs exhibited more invasive and metastatic potentials both *in vitro* and *in vivo*. Patients with more OV6$^+$ tumor cells were associated with aggressive clinicopathologic features and poor prognosis. CXCR4 is expressed at higher levels in OV6$^+$ cells. Recombinant stromal cell-derived factor-1 (SDF-1) treatment expanded the OV6$^+$ HCC T-ICs population, by sustaining the stem cell property of OV6$^+$ cells. The SDF-1 effect was blocked by a specific CXCR4 inhibitor, AMD3100, or transfection of siRNA targeting CXCR4.

Conclusions: OV6$^+$ HCC cells may represent a subpopulation of T-ICs with augmented invasion and metastasis potential, which contribute to progression and metastasis of HCC. The SDF-1/CXCR4 axis also provides therapeutic targets for elimination of liver T-ICs.

Keywords: Hepatocellular carcinoma; Tumor-initiating cells; OV6; Metastasis; CXCR4.

Received 9 October 2011; received in revised form 2 April 2012; accepted 19 April 2012; available online 19 May 2012

* Corresponding author. Address: International Cooperation Laboratory on Signal Transduction, Eastern Hepatobiliary Surgery Institute/Hospital, 225 Changhai Road, Shanghai 200438, China. Tel.: +86 21 8187 5361; fax: +86 21 6556 6851.
E-mail address: hywangk@vip.sina.com (H.-Y. Wang).
† These authors contributed equally to this work.

Abbreviations: CSCs, cancer stem cells; T-ICs, tumor-initiating cells; HCC, hepatocellular carcinoma; SDF-1, stromal cell-derived factor 1; RT-PCR, reverse transcription-polymerase chain reaction.

Introduction

As the sixth most common solid cancer and the third leading cause of cancer-related mortality worldwide, HCC causes approximately 700,000 deaths yearly [1]. Despite recent advances in diagnosis and treatment of HCC, the prognosis of HCC remains dismal. The 5-year tumor recurrence rate ranges from 40% to 70%, which results from aggressive invasion and high metastasis rates [2].

Recent advances in the fields of stem cell and cancer biology have shed light on cancer stem cells (or tumor-initiating cells, T-ICs) and origin of many hematological malignancies and solid tumors [3]. It is widely accepted that cancer stem/progenitor cells exhibit self-renewing capacities and are responsible for tumor maintenance and resistance to conventional anticancer therapeutics. Similarly, recent experiments highlight the importance of T-ICs in HCC. By using CD133 [4–6], EpCAM [7], CD13 [8], CD44 [9], CD90 [10], CD24 [11] as markers of T-ICs, it has been shown that the isolated marker-positive HCC cells possess tumor-initiating capacity and self-renewal ability, generating the phenotypic heterogeneity of the parental tumor, and being more resistant to conventional chemotherapies than other cancer cells.

Increasing evidence has shown that T-ICs may not only be associated with tumor initiation and growth, but may also play a crucial role in tumor invasion and metastasis [12,13]. It is therefore essential to deeply understand the liver T-ICs in order to develop more effective therapeutic strategies.

In previous studies [14], we showed that OV6, originally classified as a hepatic progenitor cell marker, was also expressed in a subpopulation of cells with greater ability to form tumor *in vivo*

Cancer

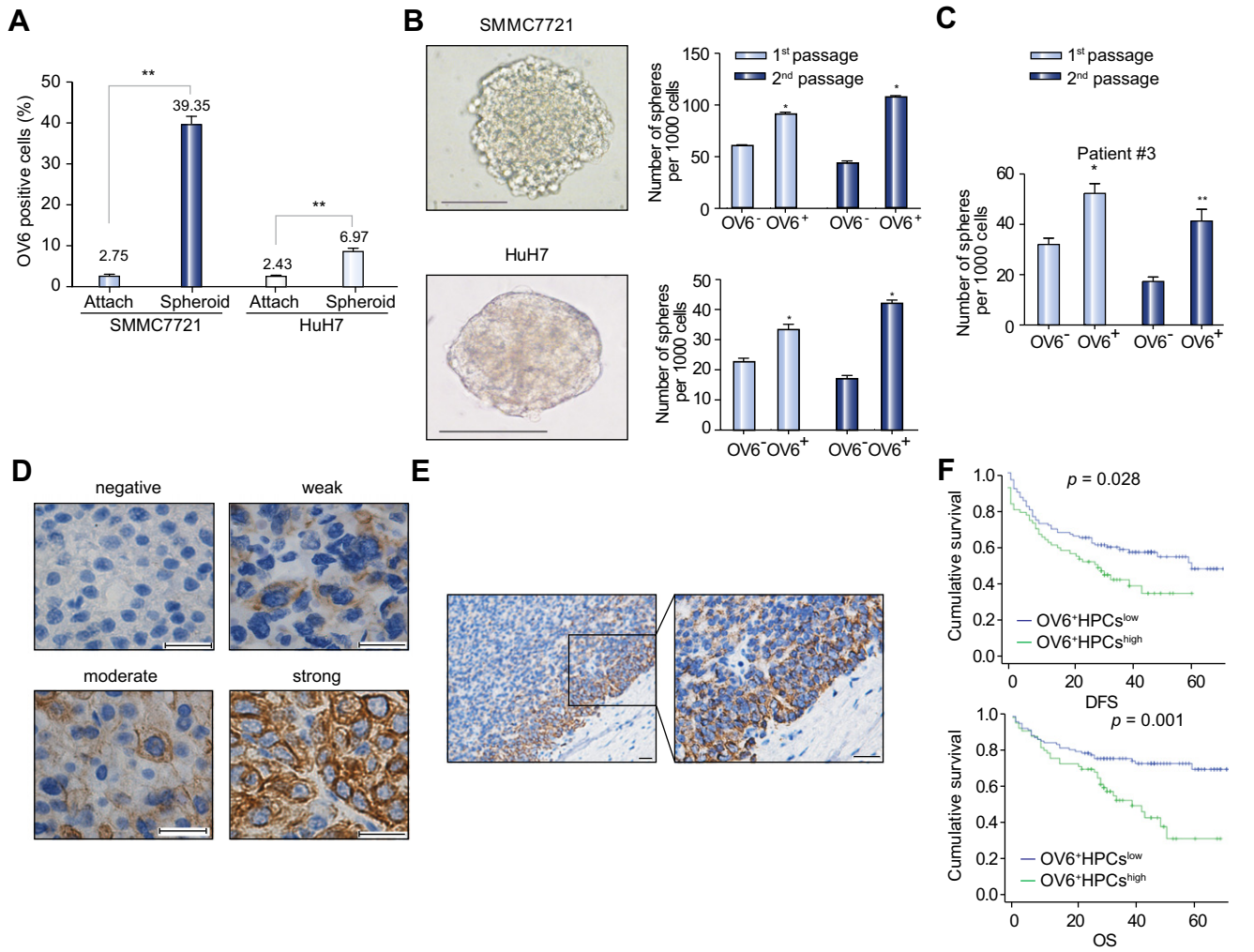

Fig. 1. Characterization of OV6$^+$ cells in HCC cell lines and a higher percentage of OV6$^+$ tumor cells indicate a poor prognosis in HCC patients. (A) Spheres established from SMMC7721 and HuH7 cells were dissociated into single cells and the percentage of OV6$^+$ cells was compared with control cells cultured in adherent conditions, by flow cytometry analysis. Experiments were performed in triplicate and data are shown as mean ± SD. (**p <0.01). (B) OV6$^+$ SMMC7721 or HuH7 cells generated more spheroids than OV6$^-$ cells. (Left panels) Representative phase-contrast images of a HCC spheroid derived from OV6$^+$ SMMC7721 or HuH7 cells. (Scale bar = 100 μm). (Right panels) Total number of spheroids from 1000 sorted OV6$^+$ cells is shown. Experiments were performed in triplicate and data are shown as mean ± SD. (*p <0.05). (C) OV6$^+$ tumor cells isolated from freshly resected HCC generate more primary and serially passaged spheroids than OV6$^-$ cells. Representative results of patient #3 are shown. (*p <0.05; **p <0.01). (D) Immunohistochemical characteristics of OV6 in HCC specimens. Representative staining of OV6 was shown as negative, weak, medium, and strong staining. Scale bar = 50 μm. (E) OV6 positive tumor cells were often located in invasive fronts of tumors. The right panel shows an enlargement of the indicated area. Scale bar = 50 μm. (F) Kaplan–Meier disease free survival (DFS) and overall survival (OS) curve of HCC patients in correlation with percentage of OV6$^+$ tumor cells. The DFS and OS rate significantly decreased in the subgroup of OV6$^+$HPCs^{high} (green line) compared with OV6$^+$HPCs^{low} (blue line). [This figure appears in color on the web.]

and substantial resistance to standard chemotherapy. However, the role of OV6$^+$ HCC tumor cells in progression and metastasis of HCC remains unclear. In this article, we report that OV6$^+$ HCC cells exhibit highly invasive and tumorigenic properties, and we also show a crucial role of SDF-1/CXCR4 axis in maintenance and migration of liver T-ICs.

Materials and methods

Histopathologic and immunohistochemical evaluation

Tissues were cut into 5-μm-thick sections and the following primary antibodies were used: mouse anti-OV6, and mouse anti-CXCR4 (R&D). Vector ABC kit (Vector Laboratories) and DAB reagent (Dako Comp) were employed in the detection procedure. All slides were observed and photographed with an Olympus microscope (IX-70 OLYMPUS, Japan). OV6 staining of the whole tissue sections was semiquantitatively graded for percentage of cells stained as not detectable (negative), <5% (weak), 5% to 30% (moderate), and >30% (strong) of tumor cells per section, evaluating five medium-power fields of each tumor tissue by two independent observers. Similarly, the staining intensities of CXCR4 were also evaluated in each sample and stratified into negative (0–5%) or positive (>5%) category.

Experimental metastasis model

Five 6-week-old NOD/SCID mice in each experimental group were injected intravenously with 5×10^4 OV6$^+$ or OV6$^-$ SMMC7721 cells through the tail vein. Eight weeks after injection, the lungs were isolated and analyzed. Macroscopic lung metastasis was detected visually and microscopic metastases were quantified under microscope after paraffin embedment and hematoxylin and eosin (H&E) staining.